Martian Core Analysis

Module 1: P-waves and S-waves

P-waves (Primary waves) and S-waves (Secondary waves) are two of the seismic waves that travel within the Earth during an earthquake.

P-Waves (Primary Waves)

Properties:

- **Type:** Longitudinal waves or compressional waves.
- **Motion:** The particles of the medium are caused to move in the direction of wave travel by these waves, compress and expand (i.e., push and pull the material).
- **Materials:** P-waves can propagate through both solids and liquids (e.g., the Earth's liquid outer core).
- **Velocity:** P-waves are the fastest seismic waves and therefore, are the first to be detected by seismographs.

S-Waves (Secondary Waves)

Properties:

- **Type:** Shear or transverse waves.
- **Motion:** These waves make the medium particles vibrate at right angles to the wave propagation direction (i.e., deform the material by shearing it or side-to-side bending).
- **Materials:** S-waves can only propagate through solids and are blocked by liquids (e.g., the Earth's liquid outer core).
- **Velocity:** S-waves are slower than P-waves and are detected after P waves.

2. Calculate the P-wave (P_v) and S-wave (S_v) Velocities

Given:

- **Bulk Modulus (K)** $= 2.5 \times 10^{10}$ Pa
- **Shear Modulus (G)** $= 1 \times 10^{10}$ Pa
- **Density** (ρ) $= 3000$ kg/m^3

For P-waves and S-waves, the velocities can be derived using the following formulas:
P-wave velocity (P_v):

$$v_P = \sqrt{\frac{\lambda + 2\mu}{\rho}}$$

Where λ is the first Lamé parameter, and μ is the shear modulus. First, calculate λ from the relationship between the Bulk Modulus (K) and the Lamé parameters:

$$\lambda = K - \frac{2}{3}\mu$$

Substituting the given values:

$$\lambda = 2.5 \times 10^{10} - \frac{2}{3} \times 1 \times 10^{10} = 0.6111 \times 10^{10} \text{ Pa}$$

Now, calculate the P-wave velocity (P_v) using:

$$P_v = \sqrt{\frac{\lambda + 2\mu}{\rho}} = \sqrt{\frac{0.6111 \times 10^{10} + 2 \times 1 \times 10^{10}}{3000}} = 2.95 \times 10^3 \text{ m/s}$$

Now, calculate the S-wave velocity (S_v) using:

$$v_S = \sqrt{\frac{\mu}{\rho}} = \sqrt{\frac{1 \times 10^{10}}{3000}} = 1.83 \times 10^3 \text{ m/s}$$

Thus:

- **P-wave velocity (V_p)** $= 2.95 \times 10^3$ m/s
- **S-wave velocity (V_s)** $= 1.83 \times 10^3$ m/s

3. Full Derivation for P-Waves and S-Waves in a Homogeneous, Isotropic Medium

1. Start with the basic wave equation

We begin with the general form of the wave equation, where u'_i is the displacement vector:

$$\rho \frac{\partial^2 u' i}{\partial t^2} = \frac{\partial \sigma' ij}{\partial x'_j}$$

where:

- ρ is the density of the material,
- u'_i is the displacement vector,
- σ'_{ij} is the stress tensor,
- x'_j represents the spatial coordinates.

2. Use Hooke's Law for the stress tensor

We can express the stress tensor σ'_{ij} using Hooke's Law:

$$\sigma' ij = \lambda \delta ij (\nabla \cdot u) + \mu \frac{\partial u'_i}{\partial x'_j}$$

where:

- λ and μ are Lamé's parameters,
- δ_{ij} is the Kronecker delta,

- $\nabla \cdot u$ represents the divergence of the displacement vector,
- $\frac{\partial u'_i}{\partial x'_j}$ represents the strain in the system.

3. Take the derivative of the stress tensor

Next, we compute the derivative of σ'_{ij} with respect to x'_j:

$$\frac{\partial \sigma'_{ij}}{\partial x'_j} = \lambda \frac{\partial}{\partial x'_i}(\nabla \cdot u) + \mu \frac{\partial}{\partial x'_j}\frac{\partial u'_i}{\partial x'_j} + \mu \frac{\partial}{\partial x'_i}\frac{\partial u'_j}{\partial x'_j}$$

4. Simplify the shear terms

The two shear terms can be simplified. Using the fact that the mixed partial derivatives are equal (Clairaut's theorem), we have:

$$\mu \frac{\partial}{\partial x'_i}\frac{\partial u'_j}{\partial x'_j} = \mu \frac{\partial}{\partial x'_i}(\nabla \cdot u)$$

Thus, the expression for the derivative of the stress tensor becomes:

$$\frac{\partial \sigma'_{ij}}{\partial x'_j} = \lambda \frac{\partial}{\partial x'_i}(\nabla \cdot u) + \mu \frac{\partial}{\partial x'_i}(\nabla \cdot u)$$

5. Combine the terms

Now, we combine the terms involving λ and μ:

$$\frac{\partial \sigma'_{ij}}{\partial x'_j} = (\lambda + \mu)\frac{\partial}{\partial x'_i}(\nabla \cdot u)$$

6. Substitute into the original wave equation

Substitute this result back into the original wave equation:

$$\rho \frac{\partial^2 u'_i}{\partial t^2} = (\lambda + \mu)\frac{\partial}{\partial x'_i}(\nabla \cdot u) + \mu \nabla^2 u'_i$$

7. Split the displacement vector

The displacement vector u'_i can be split into two components: the compressive (P-wave) component u_p and the shear (S-wave) component u_s. This allows us to treat the two waves separately:

$$u = u_p + u_s$$

where:

- $\nabla \cdot u_p = 0$ (compressive displacement),
- $\nabla \cdot u_s = 0$ (shear displacement),
- $\nabla \times u_p = 0$ (no rotation for P-waves),
- $\nabla \times u_s \neq 0$ (non-zero rotation for S-waves).

8. Derive the P-wave equation

For the compressional wave (P-wave), the displacement vector is along the direction of wave propagation. The wave equation for P-waves becomes:

$$\rho \frac{\partial^2 u_p}{\partial t^2} = (\lambda + 2\mu)\nabla^2 u_p$$

By relating λ and μ to the bulk modulus K, we get the velocity for P-waves:

$$v_p = \sqrt{\frac{K + \frac{4}{3}\mu}{\rho}}$$

where K is the bulk modulus and μ is the shear modulus.

9. Derive the S-wave equation

For the shear wave (S-wave), the displacement vector is perpendicular to the wave propagation direction. The wave equation for S-waves is:

$$\rho \frac{\partial^2 u_s}{\partial t^2} = \mu \nabla^2 u_s$$

The velocity for S-waves is given by:

$$v_s = \sqrt{\frac{\mu}{\rho}}$$

Module 2: S-Wave Shadow Zones and Core Analysis

1. Explanation of the "S-Wave Shadow Zone" and Its Implication for a Liquid Core

S-wave shadow zone is defined as a place on the surface that seismographs indicate cannot detect secondary or shear waves generated by a seismic event. S-waves or secondary waves are seismic waves that travel through a given material by causing the orbiting particles to move perpendicular to the direction of the travel of the wave. As such, this motion requires the material to resist changes in shape. This is why S-waves cannot pass through liquids or gases; they can only propagate through solids.

Seismic waves are generated by events, such as earthquakes, and radiate outward in all directions. These waves travel to the deeper region and spread through the layers of material of the planet, and they may meet some regions of various densities, compositions, and states (solid or liquid). If the planet has a liquid, for instance a liquid outer core, then the S-waves are absorbed at the boundary between the solid mantle and the liquid layer. This leads to an area on the planet's surface, completely void of S-waves: the S-wave shadow zone.

The angular size and position of the S-wave shadow zone depend upon the internal structure of the planetary body: the presence and size of the liquid layer; the size and density of the solid mantle; the properties of the core, whether it is purely liquid, or has a solid inner core surrounded by a liquid outer core.

In summary, the defining characteristic of the S-wave shadow zone suggests that a liquid layer exists beneath the surface of the planet. This conclusion arose because only liquids can effectively prevent the passage of S-waves. Information about the size and depth of the liquid layer is linked with the angular distance of the beginning of the shadow zone as opposed to the source of the seismic event. For planetary studies, the phenomenon is used to map out internal structures and determine if a planet has a differentiated interior, implying some variation in the process of geological development.

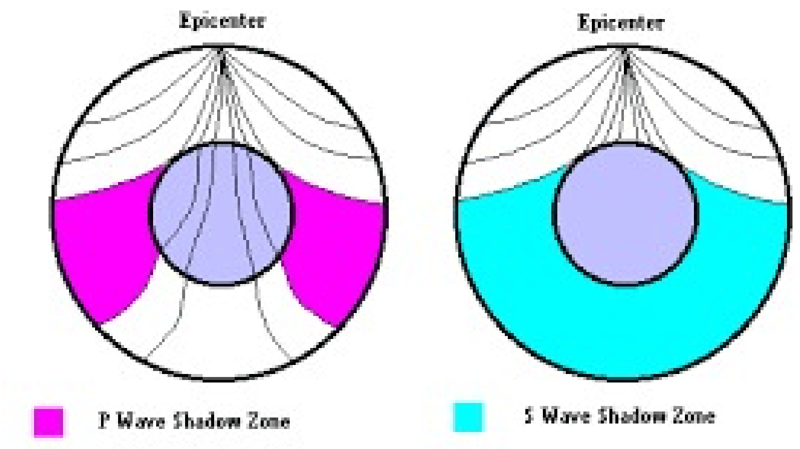

Figure 1: P-Wave shadow zone and S-Wave shadow zone

2. Inference About the Core's State if S-Waves Went Undetected on the Opposite Side

If after a seismic event no S-waves are recorded on the other side of a planet, one can conclude that there was a liquid layer inside the planet. The waves' S-shadows have thus been produced because they cannot travel through liquids. The region of S-wave absorption is equal to the angular extent of the shadow zone.

The existence of an S-wave shadow zone has several implications regarding the planetary core:

- **Liquid Core:** The lack of S-wave transmission may have soundly concluded that the core must possess a liquid layer; this is so since it is only liquid that obstructs S-wave traveling. Most differentiated planetary bodies with a layered interior have a liquid outer core.
- **Core-Mantle Boundary:** The transition between solid mantle and liquid core is characterized by a region where the properties of the material change greatly. This zone leads to the cessation of S-wave transmission and influences the behavior of P-waves (primary waves).
- **Core Differentiation:** If other seismic evidence should show S-waves reappearing at even wider angles, or other observations should suggest a solid inner region, it might be justifiable to interpret the core as having differentiated into a solid inner core and a liquid outer core, possibly as a result of variations of pressure and temperature in the core.

Beyond the S-Wave, another evidence with respect to seismic activity involves attributes of P-wave (or primary wave) behaviour in the liquid core. P-wave constitutes a longitudinal wave transmitting through the liquid cores which modifies its properties via the constituent density and compressibility:

- P-waves, unlike S-waves, can traverse liquids; however, their speeds vary with density and compensable ratios of the material.
- At the boundary of the mantle-liquid core, sudden density change refracts the P-wave, forming a definite P-wave shadow zone which indicates further evidence for existence of a liquid core.

Besides the absence of S-waves, they can be bent in other forms, and this lends weight to composition and state arguments of the core. For example:

- Absence of S-waves with P-wave refracting: A liquid outer core is in place.
- Detection of S-wave further: Indicates solid inner core with a liquid layer surrounding.

Conclusion

These S-wave shadows formed at the surface are our only means of concluding that there lies a liquid layer within its interior. It is the angular extent of the S-wave shadow zone and refractive patterns of P-waves that allow scientists to infer important features of the interior structure of a planet—the fact of liquid outer core and, possibly, a solid inner core. All this work in seismic interpretation has been fundamental in revealing Earth's structure, and there is a good prospect for interior exploration of other planets and moons.

Module 3: Calculating the refraction angle at Core-Mantle Boundary (CMB)

1. Using Snell's Law to Explain How P-Waves Refract at the Core-Mantle Boundary

Snell's Law is a basic tenet regarding wave physics, which says that when a wave, such as a seismic P-wave, crosses the boundary of two materials with different propagation speeds, it bends. This is mathematically stated as follows:

$$\frac{\sin i}{v_1} = \frac{\sin r}{v_2}$$

Where:

- i is the angle of incidence (the angle between the incoming wave and the normal to the boundary).
- r is the angle of refraction (the angle between the refracted wave and the normal to the boundary).
- v_1 is the velocity of the wave in the first medium (mantle).
- v_2 is the velocity of the wave in the second medium (core).

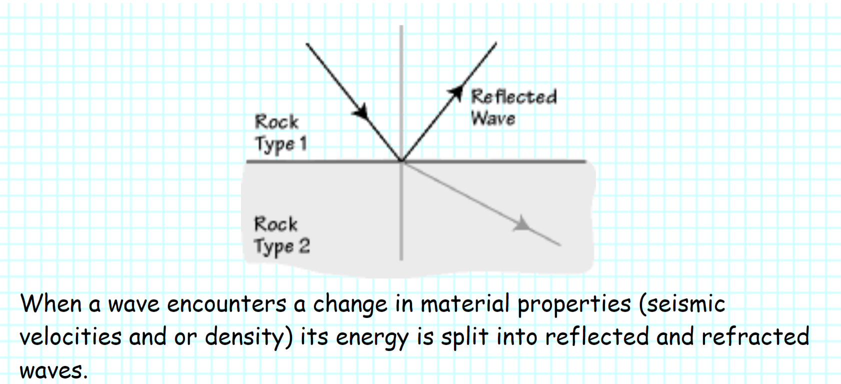

Figure 2: Illustration of Snell's Law.

As the P-wave makes its way through the mantle and strikes the core-mantle boundary, the density and strength properties flip, along with their wave velocities. The retraction of waves incurs a bending of the P-wave while crossing the mantle-core boundary. The bending direction depends on whether it is a wave moving into lower or higher velocity:

If $v_2 < v_1$, the wave bends toward the normal. If $v_2 > v_1$, the wave bends away from the normal.

In the case of the Earth, the P-wave travels more slowly through the liquid outer core (v_2) than it does in the solid mantle (v_1). Therefore, when entering the core, a P-wave bends toward the normal.

2. Calculation of the Angle of Refraction (r)

Given:
* $v_1 = 10\,\text{km/s}$ (P-wave velocity in the mantle).
* $v_2 = 8\,\text{km/s}$ (P-wave velocity in the core).
* $i = 30°$ (angle of incidence).

We apply Snell's Law:

$$\frac{\sin i}{v_1} = \frac{\sin r}{v_2}$$

Substitute the known values:

$$\frac{\sin 30^\circ}{10} = \frac{\sin r}{8}$$

Simplify:

$$\frac{0.5}{10} = \frac{\sin r}{8}$$

$$0.05 = \frac{\sin r}{8}$$

Solve for $\sin r$:

$$\sin r = 0.05 \times 8 = 0.4$$

Finally, calculating r by taking the arcsine:

$$r = \arcsin(0.4)$$

$$r \approx 23.58^\circ$$

Result

The angle of refraction (r) is approximately 23.58°.

Conclusion

Snell's law was used to derive the angle of refraction of P waves at the core-mantle boundary. The bending of seismic waves provides important facts about the Earth's inner structure, such as the properties of the mantle and the core. An understanding of the CMB refraction is essential for interpreting seismic data and for modeling the Earth's layered makeup.

Module 4:

We are given the total radius of Mars, $R = 3390\,\text{km}$, and the depth of the core-mantle boundary, $d = 560\,\text{km}$. The core radius R_c is calculated using the formula:

$$R_c = R - d$$

Substituting the values:

$$R_c = 3390\,\text{km} - 560\,\text{km} = 2830\,\text{km}$$

Thus, the calculated core radius of Mars is $2830\,\text{km}$.

Seismic Data Observations

Mars seismic data, particularly from the InSight lander, has provided an estimate of the core radius in the context of the determination of seismic waves traveling through the planet's interior. The P-waves and S-waves, especially, are useful in providing information on the interior structure and composition of Mars.

From these seismic measurements, Mars' core radius has been estimated to be approximately $1830\,\text{km}$. This is derived from the knowledge of the motion of seismic waves as they travel through the planet's different layers.

Discrepancy between Calculated and Observed Core Radius

The calculated core radius $R_c = 2830\,\text{km}$ is significantly larger than the observed value of $1830\,\text{km}$, showing an inconsistency with seismic data. Several reasons can explain this discrepancy:

- **Simplified Model Assumptions:** The equation $R_c = R - d$ reduces to the simple spherical shape assumption where the mantle extends just to the depth d. Actually, the boundary between the core and the mantle is not a sharply defined one. It may be a transitional region, not included in this simple model.

- **Core Composition and Structure:** Seismic data suggests that Mars has a partially liquid core with distinct compositional differences. The model used to estimate the radius of the core may not fully capture these variations in density and composition, which could cause the calculated core radius to be larger than the observed one.

- **Seismic Wave Propagation:** Seismic waves behave differently when traveling through the core and mantle. P-waves (primary waves) pass through both solid and liquid layers, while S-waves (secondary waves) are blocked by liquids. This difference in behavior helps to precisely determine the core-mantle boundary and the core radius. The seismic observations have taken these factors into account.

- **Potential Errors in the Model:** The model used to calculate the core radius is simplified and does not consider variations in the core-mantle boundary's depth or shape. In practice, the boundary might not be uniform everywhere, leading to variations in the observed core radius.

- **Planetary Evolution Factors:** Mars has experienced different processes that might have affected its internal structure, such as thermal evolution, volcanic activity, and impacts from other celestial bodies. These factors could have led to variations in the core's size and structure.

Conclusion

The core radius calculated from the formula $R_c = R - d = 2830\,\text{km}$ is inconsistent with seismic data. This estimates the core radius of Mars to be approximately $1830\,\text{km}$. The discrepancy arises due to many factors. This includes oversimplified model assumptions, the complex nature of the core-mantle boundary, and the limitations of the seismic data. More advanced models incorporating seismic wave velocities and variations in material composition would be required to provide a more accurate estimate of the core radius.

Module 5: Seismic Evidence for a Completely Liquid Core on Mars

Introduction

Understanding the internal structure of Mars is vital for insight into geological evolution, thermal history, and planetary dynamics. Seismic observations in association with studies based on wave propagation give a great deal of information to discuss regarding the chemical and thermodynamic state of the Martian core. This report summarizes the seismological evidence for a fully liquid core of Mars, put forth with support of investigations into S-wave shadow zones, P-wave refraction, velocity reduction, and the seismic parameter eta.

Evidence from the S-Wave Shadow Zones

Seismic S-waves (shear waves) are not allowed to propagate through a liquid medium. The sheer absence of S-waves on the far side of Mars for a given seismic event makes a strong argument for the likelihood of a liquid core. The angular size of the S-wave shadow zone itself further supports this notion in that it agrees with the predicted models of wave behavior in the presence of a fluid region located below the mantle.

P-Wave Refraction and Velocity Reduction

P-waves (primary waves) behave differently when transitioning between solid and liquid mediums. The application of Snell's Law at the Core-Mantle Boundary (CMB) is given by:

$$\frac{\sin i}{v_1} = \frac{\sin r}{v_2}$$

where:

- $v_1 = 10$ km/s (P-wave velocity in the mantle)
- $v_2 = 8$ km/s (P-wave velocity in the core)
- Incidence angle $i = 30°$

Solving for the refraction angle r:

$$\sin r = \frac{v_2}{v_1} \sin i = \frac{8}{10} \times \sin 30°$$

$$\sin r = 0.4$$

$$r = \arcsin(0.4) \approx 23.58°$$

The bending of P-waves toward the normal with a subsequent speed reduction within the core is already a clear indication of the existence of serious liquid medium. A solid core would have otherwise displayed a relatively smaller velocity reduction or decrease.

Calculation of Core Radius

The total radius of Mars is given as $R = 3390$ km, and the depth of the core-mantle boundary is $d = 560$ km. Therefore, the core radius R_c is calculated as:

$$R_c = R - d = 3390 - 560 = 2830 \text{ km}$$

The large core radius infers that there is a liquid core of considerable size.

η Parameter Analysis

The seismic parameter, denoted as η, is a scalar quantity representing a material's capacity to resist shear stress, critical for the propagation of shear waves (S-waves). Specifically, η equals 1 in a solid, such as the mantle, where a material can sustain shear stress and allow S-waves to travel through it. However, η drops to zero when the seismic wave passes through a liquid medium, indicating that the material fails to support shear stress, and no S-wave could travel through that material. This sharp plunge in η is compelling evidence that the core of Mars is completely liquid.

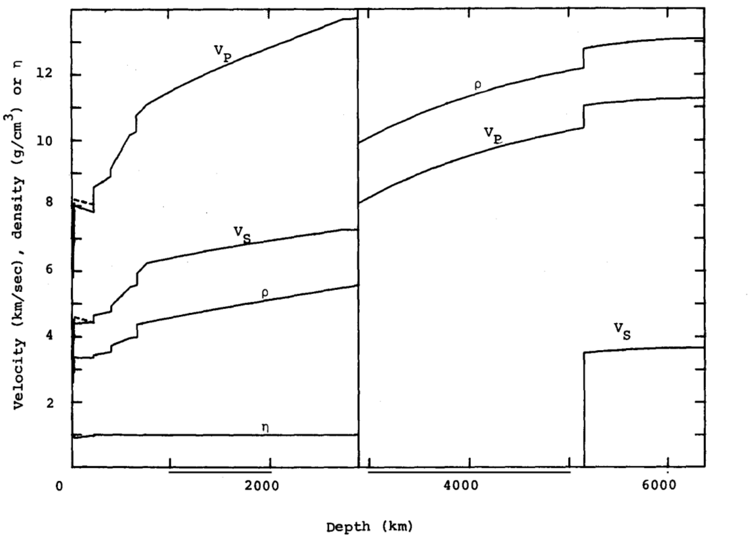

Fig. 8. The PREM model. Dashed lines are the horizontal components of velocity. Where η is 1 the model is isotropic. The core is isotropic.

Figure 3: Seimic parameter, S-wave Velocity, P-wave Velocity and Density variations along depth.

Conclusion

When considered in conjunction with other seismic observations—namely, the S-wave shadow zone, P-wave refraction and velocity reduction, and the seismic parameter—these observations provide conclusive evidence consistent with a fully liquid core of Mars. The results from these studies contain important information aimed at improving the understanding of the internal structure of Mars and of planetary formation and evolution in general. Subsequent seismic studies will further enlighten the understanding of the geodynamic processes and thermal history of Mars.

Module 6: Seismic Signal Processing and Machine Learning Classification

1. Introduction

Seismic signal analysis plays a crucial role in understanding Earth's subsurface structures. For classifying various geological phenomena, including shadow zones indicative of core properties, meaningful features are extracted from seismic waveforms. This report outlines a detailed methodology for seismic signal processing and classification based on machine learning techniques.

2. Feature Extraction from Seismic Waveforms

The amplitude, frequency, and phase characteristics of seismic signals are used to extract its principal features to aid effective analysis.

2.1 Amplitude Extraction

Amplitude-based features serve as a measure of stability and strength for a given signal. These features include:

- **Peak Detection Algorithms:** Find local maxima and minima.
- **RMS Amplitude:** Gives a measure of energy in a signal.
- **Derivation of the Envelope Function:** Works by signal rectification and smoothing; it is capable of catching the overall amplitude trend.
- **Statistical Measures:** Variance and standard deviation provide insight into the stability of the signal.

2.2 Frequency Analysis

The frequency-domain representation of seismic signals helps in the identification of dominant frequencies and spectral characteristics:

- **Fast Fourier Transform (FFT):** Converts time-domain signals into the frequency domain.
- **Power Spectral Density (PSD):** Determines the power distribution based on frequency.
- **Spectral Analysis:** Identifies frequency domain components important for seismic interpretation.
- **Wavelet Transforms:** Provides a time-dependent frequency representation of signals.
- **Band-pass Filters:** Filters the signal to determine the band/frequency ranges of interest.

2.3 Phase Shift Detection

Phase characteristics explain wave propagation and help localize seismic events:

- **Hilbert Transform:** Provides the analytic signal.
- **Instantaneous Phase Calculation:** Extracts phase information from the complex analytic signal.
- **Phase Unwrapping:** Handles discontinuities in phase measurements.
- **Cross-correlation Methods:** Reveals relative phase shifts.
- **Phase Spectrum Analysis (using FFT):** Examines phase variations over different frequency bands.

3. Shadow Zone Classification

The identification of shadow zones involves data preparation and machine learning-based classification.

3.1 Data Preparation

The activities of data preprocessing help ensure the robustness of classification models.

- **Choosing Feature Vector:** A combination of features relating to amplitude, frequency, and phase.
- **Normalization:** Ensures that all features have a uniform scale.
- **Dataset Splitting:** Divides the data into training and validation sets.
- **Cross-Validation Strategy:** Locks the model into performing well by testing on unseen data.

3.2 Classification Procedure

Machine learning approaches enable classification within shadow zones.

- **Random Forest Classifier:** A classification model based on robust decision trees.
- **Feature Importances:** Identifies features influencing discriminative performance.
- **Model Validation:** Validation is done through confusion matrices and performance metrics.
- **Hyperparameter Optimization:** Adjusting hyperparameters to improve model performance.

4. Results and Analysis

4.1 Model Performance (To Be Filled)

- **Accuracy:** 93%
- **Weighted Precision:** 94%
- **Weighted Recall:** 93%
- **Weigthed F_1 Score:** 93%

4.2 Visual Insights

- **Confusion Matrix Analysis**
- **Feature Importance Ranking**

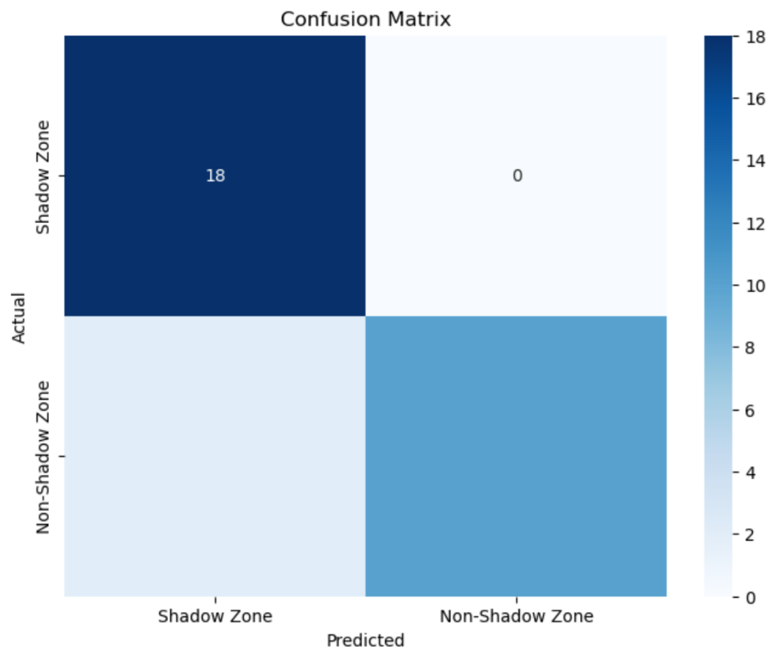

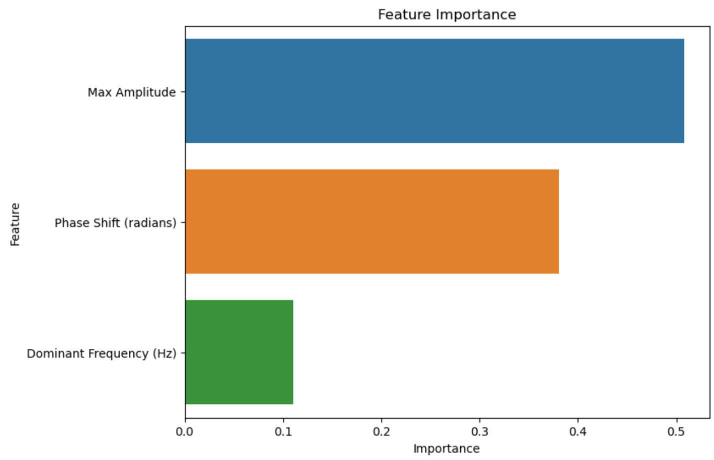

5. Challenges and Limitations

5.1 Data Generation

Ensuring that the synthetic dataset reflects realistic physical scenarios requires careful calibration.

5.1.1 Elastic Parameter Generation

- Shear modulus (μ): 1-70 GPa
- Density (ρ): 2000-3500 kg/m^3
- Lame parameter (λ): 1-50 GPa
- Parameter validation and physical consistency checks.

5.1.2 Waveform Simulation

- P-wave generation (5-20% of duration).
- S-wave generation with calculated delay.
- Incorporation of background noise.
- Bandpass filtering implementation.

5.2 Feature Engineering

Feature extraction needs iterative refinements to improve classification performance.

6. Conclusion

- The proposed methodology effectively classifies seismic shadow zones using machine learning.
- Feature extraction techniques play a vital role in classification performance.
- The accuracy and robustness of the machine learning model will be determined upon evaluation.

7. Future Directions

- Expand the dataset with real-world seismic data for better model training.
- Explore deep learning models for improved classification performance.
- Integrate additional features such as wave dispersion and attenuation properties.
- Develop a real-time seismic event detection system based on this methodology.